Effects of Ab501 (certolizumab mice equivalent) in arthritis induced bone loss

Vidal B[1], Finnilä MAJ[2,3], Lopes IP[1], Cascão R[1], Fonseca JE[1,4]

[1] Instituto de Medicina Molecular-João Lobo Antunes, Faculdade de Medicina, Universidade de Lisboa, Centro Académico de Medicina de Lisboa, Portugal;

[2] Research Unit of Health Sciences and Technology, Faculty of Medicine, University of Oulu, Oulu, Finland;

[3] Biocenter Oulu, University of Oulu, Oulu, Finland;

[4] Serviço de Reumatologia e Doenças Ósseas Metabólicas, Hospital de Santa Maria, Unidade Local de Saúde de Santa Maria, Centro Hospitalar Universitário Lisboa Norte, Centro Académico de Medicina de Lisboa, Portugal

Correspondence to

Bruno Vidal

E-mail: vidal.bmc@gmail.com

Submitted: 30/07/2024

Accepted: 02/10/2024

Abstract

Introduction - Rheumatoid arthritis (RA) is a chronic immune-mediated inflammatory disease, which causes local and systemic bone damage. The main goal of this work was to analyse, how treatment intervention with Ab501 (certolizumab mice equivalent) prevents the disturbances on bone structure and mechanics induced by arthritis.

Methods – Thirty DBA/1 collagen-induced arthritis (CIA) mice were randomly housed in experimental groups, as follows: arthritic untreated (N=9), preventive intervention (N=10) and treatment intervention (N=11). A non-induced group (N=5) was used as a control. Mice were monitored during 70 days after disease induction for the inflammatory score, ankle perimeter and body weight. After 70 days of disease progression mice were sacrificed and bone samples were collected for histology, micro-computed tomography (µCT) and 3-point bending analysis. In addition, blood samples were also collected for bone turnover markers quantification.

Results - Results showed that Ab501 administration was able to control and abrogate disease development both in preventive and early therapeutic intervention. µCT results revealed that Ab501 was able to preserve trabecular bone structure when delivered before arthritis induction.

Conclusion - Ab501 preventive administration was able to control inflammation and prevent the degradative effects of arthritis on trabecular bone structure in a CIA DBA/1 mice model.

Keywords: Animal model; Anti-TNF; Bone; Inflammation; Rheumatoid arthritis.

Introduction

Rheumatoid arthritis (RA) is a chronic immune-mediated inflammatory disease, which affects around 1% of the world-population[1]. As RA progresses there is marked bone destruction, with radiological evidence of bone erosion within 2 years of disease onset[2, 3]. In addition, osteoporosis is a common finding in patients with RA[4]. This is responsible for high rates of vertebral and hip fractures in these patients[5, 6]. RA is associated with an increased expression of the receptor activator of nuclear factor kappa–B ligand (RANKL) and low levels of its antagonist, osteoprotegerin (OPG)[7]. RANKL is a crucial activator of osteoclastogenesis[8]. In addition, RA serum and synovial fluid present an inflammatory cytokine profile, including interleukin (IL) 1β, IL6, IL17 and tumour necrosis factor (TNF), which further favors osteoclast differentiation and activation since the early phase of the disease[9-11].

Certolizumab Pegol (CZP) is a recombinant, humanized PEGylated Fc-free mAb that selectively targets and neutralizes soluble and transmembrane TNF (it inhibits signalling through both p55 and p75 *in vitro*)[12].

CZP is the only PEGylated TNF inhibitor (TNFi) agent and, because of its structure, may have slightly different molecular mechanisms in comparison to the other TNFi. CZP lacks an Fc region; minimizing potential Fc-mediated effects, such as immunogenicity, and may prevent the active transfer of CZP across the placenta, which could potentially translate to an improved safety profile during pregnancy[12-14]. Indeed, there is now clinical evidence of the safety of CZP when used during pregnancy[15, 16]. In addition, in comparison with adalimumab and infliximab, CZP does not exhibit detrimental in vitro effects such as antibody dependent cell-mediated cytotoxicity, complement-dependent cytotoxicity, apoptosis, degranulation and loss of cell integrity[12].

Several clinical studies also demonstrated potential advantages of CZP in comparison with others TNFi, which includes rapid reduction in disease activity, and low rates of injection site reaction, which makes it a suitable alternative in patients who develop hypersensitive reaction to other subcutaneous TNFi.

Moreover, PEGylation improves the circulating half-life of the drug, which increases permeability in inflamed tissues, when compared with adalimumab and infliximab, as it is suggested by results in an arthritis mouse model using biofluorescence imaging[17].

Numerous in vitro, animal and clinical studies reported beneficial effects of TNFi on inflammation and joint erosion control[18]. Although, despite the control of inflammation, the prevention of skeletal bone damage and the consequent maintenance of its mechanical properties is still unclear. Therefore, the main goal of this work was to analyse, if treatment with Ab501 in the collagen-induced arthritis (CIA) mice model is able to control tissue and bone inflammation, and also to study for the first time the AB501 ability to prevent disturbances on bone structure and strength induced by inflammation.

Methods

Animal experimental design

Fifty DBA/1 mice from Charles River (Barcelona, Spain), ten-week-old males weighing 20 – 25 g were maintained under specific pathogen free (SPF) conditions.

Animals were ordered when they were 6 weeks old and were randomly housed as follow: arthritic untreated (N=15), preventive intervention with Ab501 2 days before arthritis induction (N=15), treatment intervention upon arthritis onset with Ab501 (N=15) and a non-induced group (N=5) was used as a control. Animals were housed in standard laboratory conditions (at 22°C under 12-hour light/12-hour dark conditions). To minimize animal discomfort paper shavings were used as bedding material in Double Decker GR1800 cages (Techniplast, UK) with 5 animals per cage.

CIA protocol was performed at Instituto de Medicina Molecular, Faculdade de Medicina, Universidade de Lisboa, after 4 weeks of acclimatization, with the the sample size in each group was calculated using free sample size calculating G*Power V.3.1.9.2 software (type of power analysis: a priori; alpha (α) error probability: 0.05; power (1-beta (β) error probability): 0.95; effect size d: 1.526112; actual power: 0.9576654) [19].

The total number of animals ordered (N=50) exceeded the calculated sample size (11 animals per CIA group and 5 healthy controls) to account for potential losses. In this model, some animals do not survive the arthritis induction protocol due to technical issues, resulting in mice embolism. Additionally, because the penetrance of arthritis in the DBA/1 mice model using the CIA method is not 100% some animals in the CIA groups that do not show inflammatory signs have to be excluded from the study.

CIA induction kit for DBA/1 mice from Hook Laboratories (Lawrence, USA), according to the provider's instructions.

In accordance with Directive 2010/63/EU, all animal procedures were approved by the institutional animal welfare body (ORBEA-iMM) and licensed by the Portuguese competent authority (DGAV – Direcção Geral de Alimentação e Veterinária, license number: 0421/000/000/2016).

Immunization was performed at day 0 and the boost at day 21. A volume of 0.05 mL was injected at the base of the tail. During this period the blood vessels in the tail were dilated as a result of the initial immunization. The tail area for the booster injection was on the opposite side of the tail from the initial immunization and the dispense of the emulsion was very slow. This animal model is well characterized and generally disease onset occurs between days 16 – 35 after immunization. Highest disease activity and severity occurs at day 60 and plateaus up to day 70 post disease induction. After this period inflammatory signs start to disappear[20, 21]. At the end of the experimental period, animals that did not develop arthritis were excluded from the arthritic untreated (5) and from the treatment intervention groups (3).

In order to replicate the penetrance rate of this animal model observed in the other experimental groups, three animals with no inflammatory signs were randomly excluded from the preventive intervention group.

In addition, 4 animals died during the CIA induction protocol (1 in the arthritic untreated group, 1 in the treatment intervention group and 2 in the preventive intervention group), which decreased the final number of animals to thirty-five DBA/1 mice as follows: arthritic untreated (N=9), preventive intervention (N=10), treatment intervention (N=11) and non-induced group (N=5).

Ab501 is a non-commercialized certolizumab mice equivalent, an in-house murinised rabbit anti-mouse TNF monoclonal antibody, which was developed and provided by UCB Pharma, UK.

Preventive intervention was started two days before disease induction, with a dose of 100mg/kg/twice a week, intraperitoneally. Animals were sacrificed 70 days after disease induction (with 72 days of treatment) by CO2 narcosis.

Treatment intervention, upon arthritis onset, was started immediately after the first inflammatory signs, with a concentration of 100mg/kg/twice a week. The first administration was given intravenous, and the following ones were given intraperitoneally. The intervention rout strategy was indicated by UCB Pharma, based in previous results during the Ab501 development. Treatment was kept until disease reached the plateau and after 30 days under Ab501 treatment mice were sacrificed by CO2 narcosis.

The inflammatory score and body weight were measured during the study period. Inflammatory signs were evaluated by counting the score of each joint in a scale of 0 – 4 (0 - Normal paw; 1 - One toe inflamed and swollen; 2 - More than one toe inflamed and swollen; 3 - Entire paw inflamed and swollen; 4 - Very inflamed and swollen paw or ankylosed paw). The total score of each animal was defined as the sum of the partial scores of each affected joint. Mice were sacrificed at the end of the experimental time and blood, paws and bone samples were collected.

Histological evaluation of hind paws

We performed histological analyses of mice hind paws because this is the anatomical region which expresses the most exuberant inflammatory signs of the disease in this model. Using routine haematoxylin and eosin staining, we were able to analyse the impact of inflammation on paw structures at a microscopic level. Despite the good qualitative analysis that can be obtained with haematoxylin and eosin, a quantitative data analysis is required for objective comparisons. Left hind paw samples collected at the time of sacrifice were fixed immediately in

10% neutral buffered formalin solution and then decalcified in 10% formic acid. Samples were then dehydrated and embedded in paraffin, serially sectioned at a thickness of 5 µm. Sections were rehydrated with decreased ethanol concentrations, and then a haematoxylin and eosin staining took place. The next step was the dehydration of sections with increased ethanol concentrations.

After the clarification with Xylene (Merck KGaA, Darmstadt, Germany), a drop of Entellan (Merck KGaA, Darmstadt, Germany) was added and the coverslip applied on the biological tissue. Haematoxylin and eosin staining allow a histopathological evaluation of structural changes and cellular infiltration.

The evaluation was performed by two investigators blinded to the experimental scheme using 4 semi-quantitative scores:

• Sublining layer infiltration score (0—none to diffuse infiltration; 1—lymphoid cell aggregate; 2—lymphoid follicles; 3—lymphoid follicles with germinal center formation);

• Bone erosion score (0—no erosions; 1—minimal; 2—mild; 3—moderate; 4—severe);

• Cartilage surface (0 –normal; 1 – irregular; 2 – clefts; 3 – clefts to bone);

• Global severity score (0—no signs of inflammation; 1—mild; 2—moderate; 3—severe)[27].

Scoring was done by a single blinded observer, using a Leica DM2500 (Leica Microsystems, Wetzlar, Germany) microscope. The microscope was equipped with a color camera with a magnification of 100 and 200X that was used to acquire the images presented in this paper.

Bone remodeling markers quantification

Bone turnover markers offer information on the balance between bone formation and bone resorption. We have used the most accepted markers of bone formation (Amino terminal propeptides of type I collagen, P1NP) and resorption (Carboxy-terminal telopeptide of collagen I, CTX-I) in the context of these type of studies[22-24].

Serum samples were collected at sacrifice and stored at -80°C. Bone remodeling markers, CTX-I and P1NP, were quantified by Serum Rat Laps ELISA assay (Immunodiagnostic Systems Ltd, Boldon, UK) following strictly provider's recommendations.

For all biomarkers standard curves were generated by using reference biomarker concentrations supplied by the manufacturers. Samples were analysed using a plate reader Infinite M200 (Tecan, Mannedorf, Switzerland).

Micro-computed tomography (micro-CT) analysis

The Micro-computed tomography (micro-CT) technique was used to offer a quantitative analysis of bone quality, such as bone volume, trabecular number, surface density, among others. This technique is a standard approach to evaluate skeletal bone quality[22-26].

Structural properties of the trabecular and cortical tibiae were determined with a micro-CT system (SkyScan 1272, Bruker microCT, Kontich, Belgium). Bones were wrapped in Phosphate buffered saline (PBS) moist paper and fixed in sample holder to prevent drying and movement during the scanning. The x-ray tube was set to 50kV and beam was filtered with a 0.5mm aluminum filter. Sample position and camera settings were set to provide 5.0µm isotropic pixel size and projection images were collected every 0.45°. Tissue mineral density values were calibrated against hydroxyapatite phantoms with densities of 250mg/cm^3 and 750mg/cm^3. Reconstructions were done with NRecon (v 1.6.9.8; Bruker µCT, Kontich, Belgium) where appropriate corrections to reduce beam hardening and ring artifacts were applied. The growth plate was used as an anatomical landmark and structural properties were analysed after 50 and 800 slices for trabecular and cortical bone, respectively. Volumes of interest were collected over 200 slices by manual segmentation and shrink-wrap functions for trabecular and cortical bone, respectively. Prior to analyses of bone morphology global threshold and despeckle functions were used. Analyses were performed in agreement with guidelines for assessment of bone microstructure in rodents using micro-CT[28].

Bone mechanical tests

To complement micro-CT evaluation, we assessed the bone mechanical competence, by using the three-point flexural tests. This technique is a standard approach to evaluate skeletal bone quality[22-26].

Femurs were subjected to a 3-point bending test using a universal materials testing machine (Instron 3366, Instron Corp., Massachusetts, USA). Femurs were placed horizontally, anterior side upwards, on a support with a span length of 6.5mm. The load was applied with a constant speed of 0.155mm/s until failure occurred. Stiffness was analysed by fitting first-degree polynomial function to the linear part of recorded load deformation data. A displacement of 0.15µm between the fitted slope and the measured curve was used as criteria for yield point, whereas the breaking point was defined when the force reached maximal value. Force, deformation and absorbed energy were defined at both yield and at the breaking point.

Statistical analysis

Statistical differences were determined with Mann Whitney U test using GraphPad Prism (GraphPad, California, USA). Data were expressed as median with interquartile range. Differences were considered statistically significant for $p<0.05$.

Results

Ab501 effectively reduced inflammation in the CIA mice model of arthritis

Results showed that Ab501 administered 100mg/kg/twice a week was able to control and abrogate disease development in comparison with untreated arthritic mice (Figure 1). Untreated animals showed disease progression when compared with both intervention groups.

Ab501 abrogates local joint inflammation and local bone and cartilage damage in CIA mice.

To evaluate the effect of Ab501 treatment in the preservation of joints structure and periarticular bone, paw sections stained with haematoxylin, and eosin were performed (illustrative images can be observed in Figure 2 A-H). The histological evaluation using 4 semi-quantitative scores is depicted in Figure 2 (I-L). Untreated arthritic animals as compared to healthy controls had higher joint inflammatory infiltration (I) ($p=0.0005$), cartilage damage (J) ($p=0.0005$) and bone erosions (K) ($p=0.0005$). Sublining layer inflammatory infiltration (I) was significantly lower in arthritic animals exposed to Ab501 either in a preventive strategy ($p=0.0002$) or as an early treatment intervention ($p=0.0013$), when compared with the untreated arthritic group. Ab501 was also effective in preventing cartilage damage (J) (preventive ($p= 0.0002$) and early treatment ($p<0.0001$) strategies) and bone erosions (K) (preventive ($p<0.0001$ and early treatment ($p<0.0001$) strategies) when compared to untreated arthritic animals.

Reflecting all these features, untreated arthritic animals had higher global severity score (L) when compared with the healthy control ($p=0.0010$), and with the preventive ($p<0.0001$) and early treated ($p<0.0001$) groups.

Ab501 reduced P1NP

Biochemical markers were quantified in order to evaluate the impact of arthritis on bone metabolism. CTX-I (Fig. 3A) was slightly increased in the preventive group (p= 0.0431) when compared to healthy animals. No other statistical differences were recorded related to CTX-I quantification. P1NP (Fig. 3B) showed a significant decrease in the early treated group, when compared to untreated arthritic animals (p=0.0062).

Ab501 prevented bone structural degradation

The effect of Ab501 on inflammation-induced bone loss was assessed by µCT of trabecular (Fig 4 and 5 A - D) and cortical bone tibia (data not shown).

Results demonstrated a decreased bone volume (A), trabecular number (B) and surface density (D) in the untreated arthritic group when compared to the healthy control group (p=0.0242, p=0.0364 and 0.0364, respectively). Porosity (C) was increased in the arthritic group when compared to healthy controls (p=0.0242).

Ab501 preventive intervention was able to rescue trabecular bone integrity and trabecular bone properties in treated mice (Fig. 4 and 5). Results demonstrated that preventive Ab501 intervention was able to preserve bone structural properties, promoting the maintenance of bone volume, trabecular number and surface density. Results showed increased bone volume (A), trabecular number (B) and surface density (D) when compared to untreated arthritic animals (p=0.0002, p=0.0027 and p=0.0006, respectively). In addition, this group had also decreased values of trabecular porosity (C) when compared to untreated arthritic animals (p=0.0002). The Ab501 early treated group demonstrated no statistical differences when compared with the untreated arthritic group. Cortical bone assessed by µCT did not show any differences between experimental groups.

Three-point bending tests

There were no statistically significant differences in bone mechanical properties between the study groups (data not shown).

Discussion

During the last decades the effects of several TNF antagonists were widely studied[29]. However, this is the first publication assessing the preventive effect of an anti TNF treatment on skeletal bone in the context of an animal model of arthritis. Ab501 significantly reduced arthritis manifestations, synovial tissue inflammation, cartilage damage and bone erosions in both preventive and early treatment intervention.

Results showed that Ab501 administration was able to control and abrogate disease development both in preventive and early therapeutic interventions.

Results from bone turnover markers and from µCT suggest that preventive administration of Ab501 in an animal model of arthritis was able to modulate bone metabolism and preserve bone trabecular structure. The milder inflammatory signs verified in the preventive group is a consequence of the Ab501 therapeutic administration at an earlier stage of the disease development, limiting the pattern of disease progression. In previous studies from our group, we demonstrated that the therapeutic administration of several different compounds in the early stages of arthritis models led to more successful control of tissue inflammation and prevention of bone damage[27, 30].

No differences were observed between arthritic and control animals in cortical µCT and in three-point bending tests, where results are mostly cortical dependent[31-33]. Considering our previous experience in other animal models the systemic inflammation induces very early changes in bone macro and microarchitecture, and mechanical behaviour, leading, to increased bone fragility. However, the effect on cortical bone is slower to appear than in trabecular bone[22-24]. The CIA model has a milder onset of disease as compared with the AIA model[23, 34] meaning that it may need more time of arthritis duration, as is the case for instance for the SKG model[34] to have an impact on cortical bone and thus on 3 point bending test.

Conclusion

Ab501 was able to control and supress inflammatory activity, erosions and cartilage damage in the CIA mice model of arthritis. In addition, Ab501 preventive treatment was able to preserve bone trabecular structure.

Aknowledgements

The authors would like to acknowledge UCB Pharma.

Competing interests

JEF received unrestricted research grants or acted as a speaker for Abbvie, Amgen, Biogen, BMS, Janssen, Lilly, Medac, MSD, Novartis, Pfizer, Roche, UCB

The other authors have declared that no competing interests exist.

Funding

This work was supported by UCB in the context of an Investigator Initiated Study where UCB provided financial and product support.

Tables and Figures

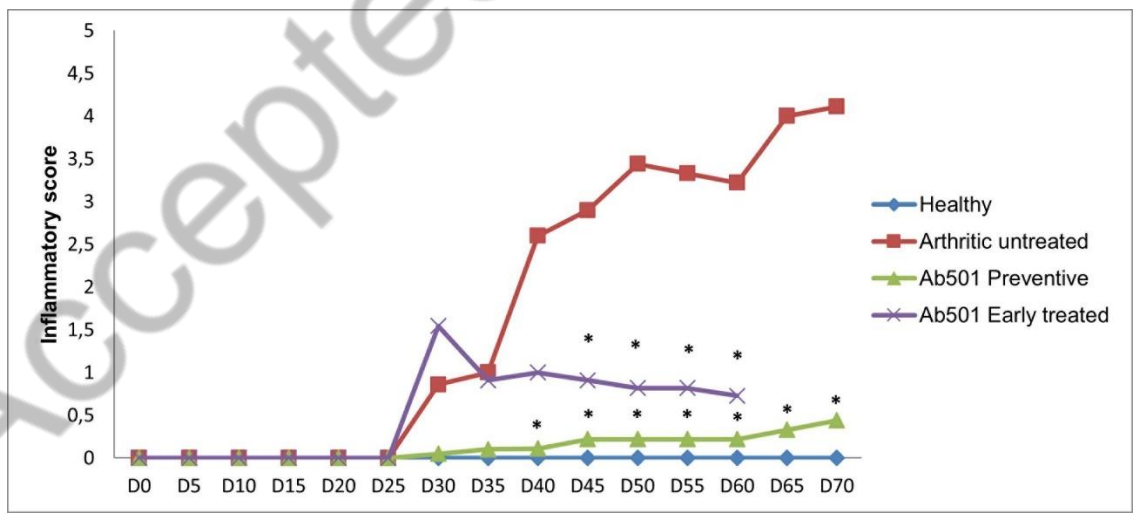

Figure 1 – Inflammatory score –Preventive and early treated groups were compared with the arthritic untreated group. Statistical differences were determined with non-parametric Mann Whitney U test using GraphPad Prism (GraphPad, California, USA). Differences were considered statistically significant for p values ≤ 0.05.

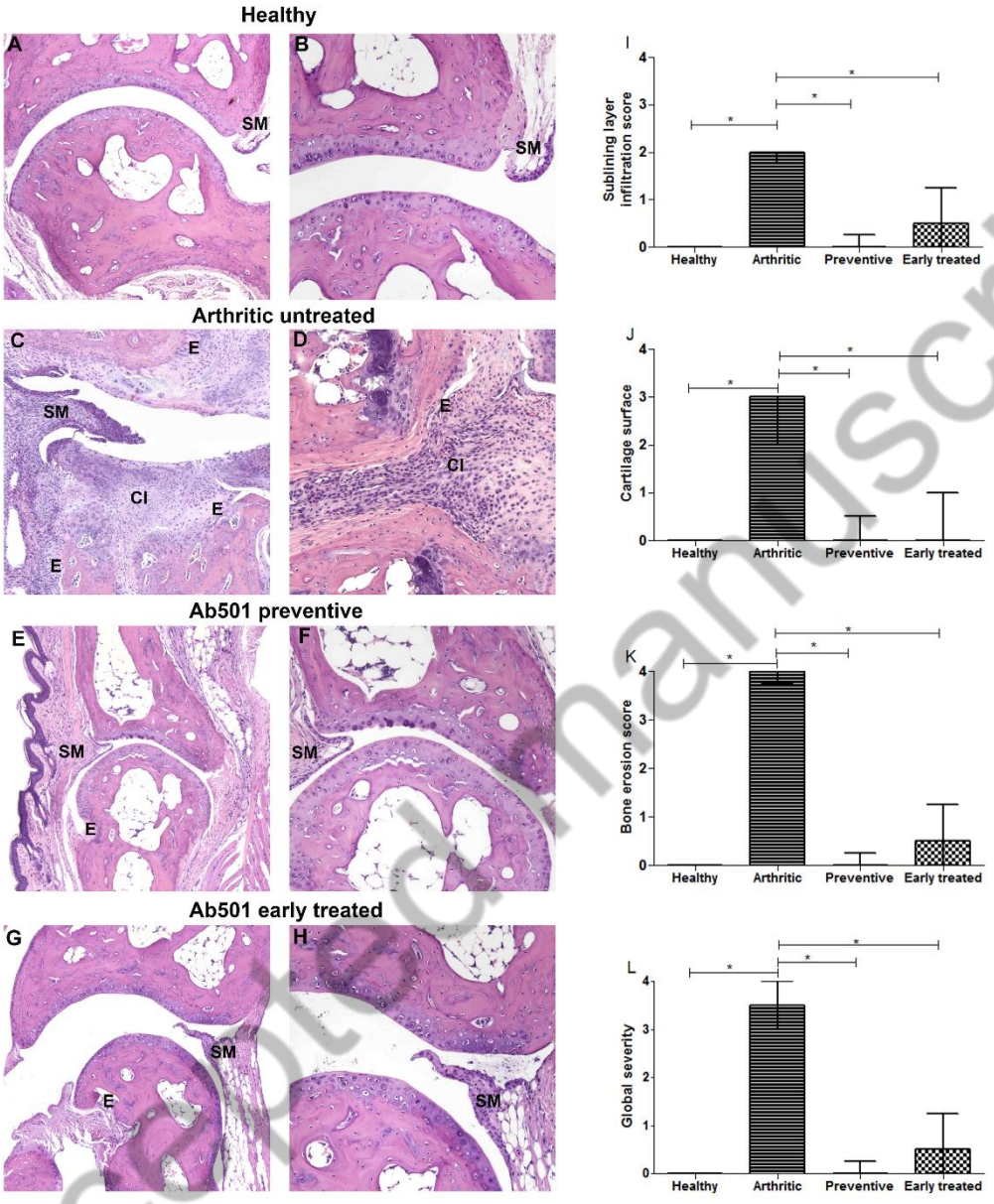

Figure 2 – Histological images of paws after Ab501 administration. These patterns are merely illustrative of the type of histological features observed. CI– cellular infiltration, E– edema or erosion, SM–synovial membrane. Left images (A; C; E; G) magnification of 100X and right images, the respective magnification of 200X (B; D; F; H). Ab501 suppresses arthritic inflammation and tissue damage locally in the joints of CIA mice. A semi-quantitative evaluation of histological sections was performed. Notice that Ab501 inhibited cellular infiltration (I) and prevented cartilage and bone erosion occurrence (J; K, respectively), allowing for a normal joint structure, comparable to healthy mice (L). Data are expressed as median with interquartile range. Differences were considered statistically significant for p-values<0.05, according to Mann Whitney U test. Healthy N=5, Arthritic untreated N=9, Preventive N=10 and Early treated N=11.

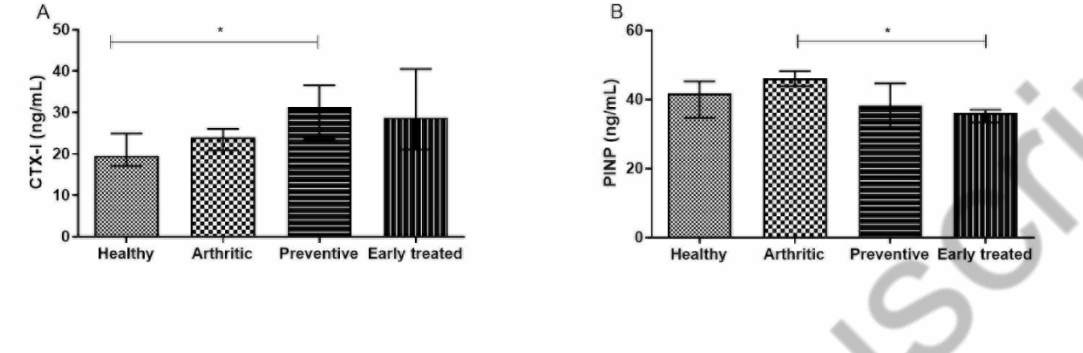

Figure 3 – Bone turnover markers quantifications. Serum samples collected at the sacrifice day were analysed by ELISA technique. Bone resorption marker CTX-I (A) was increased in the Ab501 group when compared to healthy animals (p=0.0431). P1NP (B) was decreased in the early treated therapeutic group (p=0.0062 vs arthritic animals). Data are expressed as median with interquartile range. Differences were considered statistically significant for p-values<0.05, according to Mann Whitney U test. Healthy N=5, Arthritic N=9, Preventive N=10 and Early treated N=11.

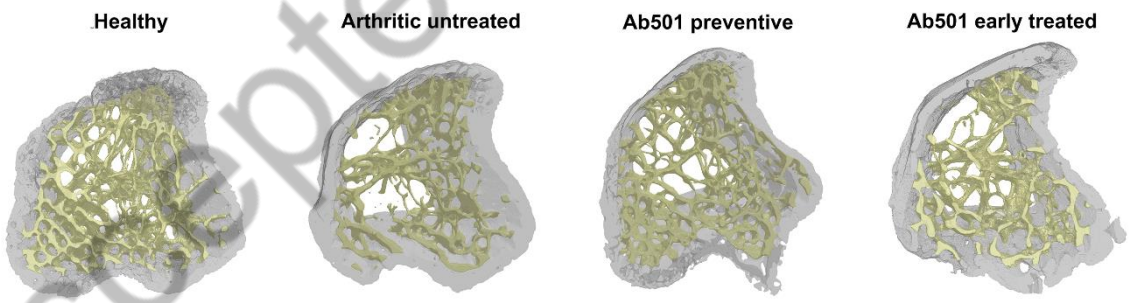

Figure 4 - MicroCT images from healthy, untreated arthritic and Ab501 preventive and early treated groups from mice tibiae. Images acquired with SkyScan 1272, Bruker microCT, Kontich, Belgium.

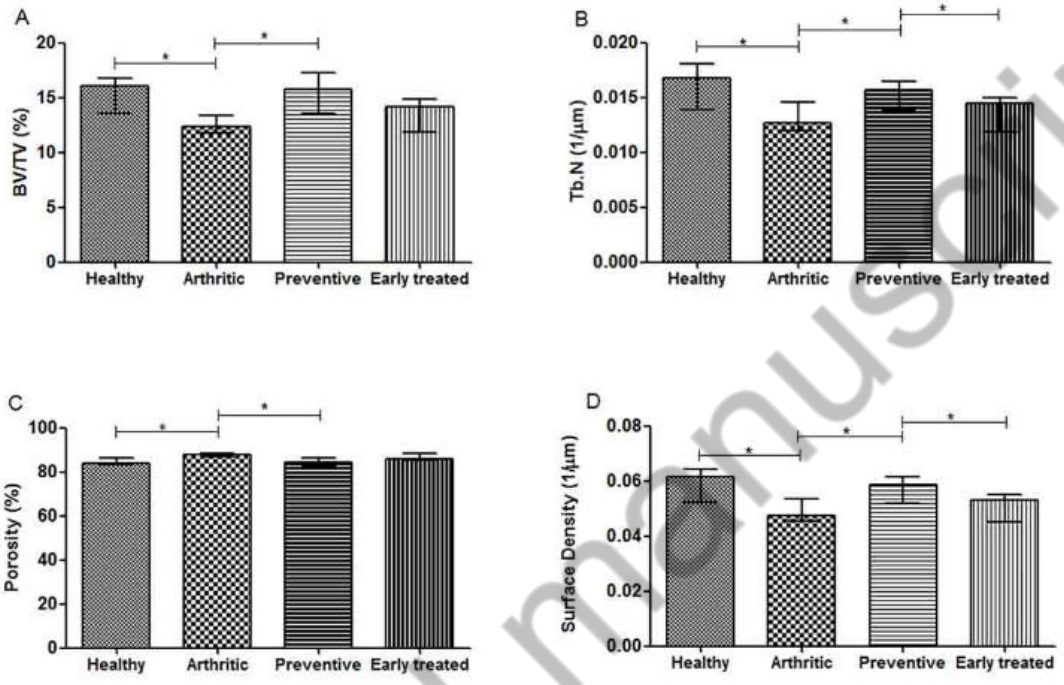

Figure 5 – Micro-computed tomography (micro-CT) analysis of tibiae mice. The Ab501 preventive group showed increased values for bone trabecular volume (A), number (B) and surface density (D) and decreased values of porosity (C) when compared to the untreated arthritic group. Differences were considered statistically significant for p-values<0.05, according to the Mann–Whitney U test. Healthy N=4, untreated arthritic N=9, Preventive N=10 and Early treated N=11.

References

1. Alamanos Y, Drosos AA. Epidemiology of adult rheumatoid arthritis. Autoimmunity reviews. 2005;4(3):130-6. https://doi.org/10.1016/j.autrev.2004.09.002

2. Yelin E, Callahan LF. The economic cost and social and psychological impact of musculoskeletal conditions. National Arthritis Data Work Groups. Arthritis and rheumatism. 1995;38(10):1351-62. https://doi.org/10.1002/art.1780381002

3. Lin YY, Jean YH, Lee HP, Chen WF, Sun YM, Su JH, et al. A soft coral-derived compound, 11-epi-sinulariolide acetate suppresses inflammatory response and bone destruction in adjuvant-induced arthritis. PLoS One. 2013;8(5):e62926. https://doi.org/10.1371/journal.pone.0062926

4. Haugeberg G, Orstavik RE, Uhlig T, Falch JA, Halse JI, Kvien TK. Bone loss in patients with rheumatoid arthritis: results from a population-based cohort of 366 patients followed up for two years. Arthritis and rheumatism. 2002;46(7):1720-8. https://doi.org/10.1002/art.10408

5. Marshall D, Johnell O, Wedel H. Meta-analysis of how well measures of bone mineral density predict occurrence of osteoporotic fractures. BMJ. 1996;312(7041):1254-9. https://doi.org/10.1136/bmj.312.7041.1254

6. Eric-Jan JA K. Bone mass in rheumatoid arthritis. CLINICAL AND EXPERIMENTAL RHEUMATOLOGY. 2000.

7. Fonseca JE, Cortez-Dias N, Francisco A, Sobral M, Canhao H, Resende C, et al. Inflammatory cell infiltrate and RANKL/OPG expression in rheumatoid synovium: comparison with other inflammatory arthropathies and correlation with outcome. Clin Exp Rheumatol. 2005;23(2):185-92.

8. Boyle WJ, Simonet WS, Lacey DL. Osteoclast differentiation and activation. Nature. 2003;423(6937):337-42. https://doi.org/10.1038/nature01658

9. Moura RA, Cascao R, Perpetuo I, Canhao H, Vieira-Sousa E, Mourao AF, et al. Cytokine pattern in very early rheumatoid arthritis favours B-cell activation and survival. Rheumatology. 2011;50(2):278-82. https://doi.org/10.1093/rheumatology/keq338

10. Cascao R, Moura RA, Perpetuo I, Canhao H, Vieira-Sousa E, Mourao AF, et al. Identification of a cytokine network sustaining neutrophil and Th17 activation in untreated early rheumatoid arthritis. Arthritis research & therapy. 2010;12(5):R196. https://doi.org/10.1186/ar3168

11. Caetano-Lopes J, Canhao H, Fonseca JE. Osteoimmunology--the hidden immune regulation of bone. Autoimmun Rev. 2009;8(3):250-5. https://doi.org/10.1016/j.autrev.2008.07.038

12. Pasut G. Pegylation of biological molecules and potential benefits: pharmacological properties of certolizumab pegol. BioDrugs. 2014;28 Suppl 1:S15-23. https://doi.org/10.1007/s40259-013-0064-z

13. Llorenc V, Mesquida M, Sainz de la Maza M, Blanco R, Calvo V, Maiz O, et al. Certolizumab Pegol, a New Anti-TNF-alpha in the Armamentarium against Ocular Inflammation. Ocul Immunol Inflamm. 2016;24(2):167-72.

14. G Fossati AN. Certolizumab pegol has a different profile from other anti-TNFs, including golimumab, in a variety of in vitro assays. Journal of translational medicine. 2010. https://doi.org/10.1186/1479-5876-8-S1-P37

15. Fechtenbaum M, Md Yusof MY, Emery P. Certolizumab pegol in rheumatoid arthritis: current update. Expert Opin Biol Ther. 2014;14(6):841-50. https://doi.org/10.1517/14712598.2014.900043

16. Curtis JR, Mariette X, Gaujoux-Viala C, Blauvelt A, Kvien TK, Sandborn WJ, et al. Long-term safety of certolizumab pegol in rheumatoid arthritis, axial spondyloarthritis, psoriatic arthritis, psoriasis and Crohn's disease: a pooled analysis of 11 317 patients across clinical trials. RMD Open. 2019;5(1):e000942. https://doi.org/10.1136/rmdopen-2019-000942

17. Palframan R, Airey M, Moore A, Vugler A, Nesbitt A. Use of biofluorescence imaging to compare the distribution of certolizumab pegol, adalimumab, and infliximab in the inflamed paws of mice with collagen-induced arthritis. Journal of immunological methods. 2009;348(1-2):36-41. https://doi.org/10.1016/j.jim.2009.06.009

18. Meroni PL, Valesini G. Tumour necrosis factor alpha antagonists in the treatment of rheumatoid arthritis: an immunological perspective. BioDrugs. 2014;28 Suppl 1:S5-13. https://doi.org/10.1007/s40259-013-0063-0

19. 2009. EP. Effect size calculators. 2009 [Available from: http://mywebpolyueduhk/mspaul/calculator/calculatorhtml.

20. Bajtner E, Nandakumar KS, Engstrom A, Holmdahl R. Chronic development of collagen-induced arthritis is associated with arthritogenic antibodies against specific epitopes on type II collagen. Arthritis research & therapy. 2005;7(5):R1148-57. https://doi.org/10.1186/ar1800

21. Laboratories H. CIA Induction in DBA/1 Mice: Hooke Laboratories; 2013 [Available from: https://hookelabs.com/protocols/ciaInduction_DBA1.html.

22. Vidal B, Cascao R, Finnila MAJ, Lopes IP, da Gloria VG, Saarakkala S, et al. Effects of tofacitinib in early arthritis-induced bone loss in an adjuvant-induced arthritis rat model. Rheumatology (Oxford). 2018;57(8):1461-71. https://doi.org/10.1093/rheumatology/kex258

23. Vidal B, Cascao R, Vale AC, Cavaleiro I, Vaz MF, Brito JA, et al. Arthritis induces early bone high turnover, structural degradation and mechanical weakness. PloS one. 2015;10(1):e0117100. https://doi.org/10.1371/journal.pone.0117100

24. Vidal B, Cascao R, Finnila MAJ, Lopes IP, Saarakkala S, Zioupos P, et al. Early arthritis induces disturbances at bone nanostructural level reflected in decreased tissue hardness in an animal model of arthritis. PLoS One. 2018;13(1):e0190920. https://doi.org/10.1371/journal.pone.0190920

25. Cascao R, Vidal B, Jalmari Finnila MA, Lopes IP, Teixeira RL, Saarakkala S, et al. Effect of celastrol on bone structure and mechanics in arthritic rats. RMD Open. 2017;3(2):e000438. https://doi.org/10.1136/rmdopen-2017-000438

26. Abdulghani S, Caetano-Lopes J, Canhao H, Fonseca JE. Biomechanical effects of inflammatory diseases on bone-rheumatoid arthritis as a paradigm. Autoimmun Rev. 2009;8(8):668-71. https://doi.org/10.1016/j.autrev.2009.02.021

27. Cascao R, Vidal B, Raquel H, Neves-Costa A, Figueiredo N, Gupta V, et al. Effective treatment of rat adjuvant-induced arthritis by celastrol. Autoimmun Rev. 2012;11(12):856-62. https://doi.org/10.1016/j.autrev.2012.02.022

28. Bouxsein ML, Boyd SK, Christiansen BA, Guldberg RE, Jepsen KJ, Muller R. Guidelines for assessment of bone microstructure in rodents using micro-computed tomography. Journal of bone and mineral research : the official journal of the American Society for Bone and Mineral Research. 2010;25(7):1468-86. https://doi.org/10.1002/jbmr.141

29. Radner H, Aletaha D. Anti-TNF in rheumatoid arthritis: an overview. Wien Med Wochenschr. 2015;165(1-2):3-9. https://doi.org/10.1007/s10354-015-0344-y

30. Cascao R, Vidal B, Lopes IP, Paisana E, Rino J, Moita LF, et al. Decrease of CD68 Synovial Macrophages in Celastrol Treated Arthritic Rats. PLoS One. 2015;10(12):e0142448. https://doi.org/10.1371/journal.pone.0142448

31. Silva MJ. Musculoskeletal Structure and Strength Core - Bone Mechanical Testing by Three-Point Bending. Washington: Washington University; 2016.

32. Oksztulska-Kolanek E, Znorko B, Michalowska M, Pawlak K. The Biomechanical Testing for the Assessment of Bone Quality in an Experimental Model of Chronic Kidney Disease. Nephron. 2016;132(1):51-8. https://doi.org/10.1159/000442714

33. Gajos-Michniewicz A, Pawlowska E, Ochedalski T, Piastowska-Ciesielska A. The influence of follistatin on mechanical properties of bone tissue in growing mice with overexpression of follistatin. Journal of bone and mineral metabolism. 2012;30(4):426-33. https://doi.org/10.1007/s00774-011-0347-8

34. Caetano-Lopes J, Nery AM, Canhao H, Duarte J, Cascao R, Rodrigues A, et al. Chronic arthritis leads to disturbances in the bone collagen network. Arthritis research & therapy. 2010;12(1):R9. https://doi.org/10.1186/ar2908